

[Regular Paper]

Effect of Cerium Addition to Bismuth–molybdenum Complex Oxide Catalyst for Partial Oxidation of Propylene to Acrolein

Shigeru SUGIYAMA^{†1)*}, Mika MIYAKE^{†2)}, Mizuho YOSHIDA^{†3)}, Yuki NAKAO^{†2)},
Naohiro SHIMODA^{†1)}, and Masahiro KATO^{†1)}^{†1)} Dept. of Applied Chemistry, Tokushima University, Minamijosanjima, Tokushima 770-8506, JAPAN^{†2)} Dept. of Chemical Science and Technology, Tokushima University, Minamijosanjima, Tokushima 770-8506, JAPAN^{†3)} Dept. of Science and Technology, Tokushima University, Minamijosanjima, Tokushima 770-8506, JAPAN

(Received February 28, 2020)

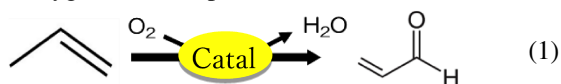
The effect of Ce addition to a Bi–Mo complex oxide catalyst supported on SiO₂ was examined on the partial oxidation of propylene to acrolein. The catalyst consisted of an oxygen-supply phase in which the lattice oxygen in Mo-oxide was doped with transition metals such as Fe, Ni and Co and was supported by SiO₂ and a catalytic-active phase that involved hydrogen abstraction from a reactant in the Bi-center of Bi–Mo oxide, which was supported by the oxygen-supply phase. In the present study, Ce was added to the oxygen-supply phase to enhance its redox nature. Ce addition was advantageous particularly under oxygen-rich conditions in the feed stream. For example, at $P(\text{C}_3\text{H}_8) = 10.1$ kPa and $P(\text{O}_2) = 15.5$ kPa at 623 K, the yield of acrolein was slightly enhanced from 57.6 % with 0 % Ce doping to 65.3 % with 20 % Ce doping at 6 h on-stream. However, under more oxygen-rich conditions at $P(\text{C}_3\text{H}_8) = 10.1$ kPa and $P(\text{O}_2) = 31.0$ kPa at 623 K, the yield of acrolein was approximately doubled from 27.7 % with 0 % Ce doping to 61.8 % with 20 % Ce doping at 6 h on-stream. Analysis using XPS of the previously used catalysts for the reaction in the absence of gaseous oxygen confirmed the unique redox behavior between the catalytic-active phase and the oxygen-supply phase as the lattice oxygen in the catalytic-active phase was replenished from the oxygen-supply phase to maintain the surface properties of the catalytic-active phase. The XPS results and the remarkable effect of Ce addition to the oxygen-supply phase under oxygen-rich conditions confirmed the validity of the concept of the catalyst preparation consisting of an oxygen-supply phase and a catalytic-active phase.

Keywords

Partial oxidation, Propylene, Acrolein, Bismuth–molybdenum oxide, Cerium doping

1. Introduction

Bismuth–molybdenum oxide was first reported as a selective catalyst for the oxidation of propylene to acrolein^{1,2)}, but has since been used for the conversion of propylene to acrylonitrile *via* a reaction with ammonia and oxygen (SOHIO process)^{3)–5)}.



Oxidation of propylene to acrolein using a doped bismuth–molybdenum oxide catalyst has been extensively studied to enhance the catalytic activity^{6)–10)}. Activity improvement was reported using Fe-doped,¹¹⁾ Co-doped¹²⁾, and V-doped¹³⁾ catalysts together with binary systems such as Fe–Co-doped¹⁴⁾ and Co–Ni-doped¹⁵⁾

bismuth–molybdenum oxide catalysts. Since bismuth–molybdenum oxide catalysts have a long history of industrial use on a large scale, this catalyst process is rarely investigated by academia. However, the involved industries have continued to actively research and develop this process^{16)–20)}.

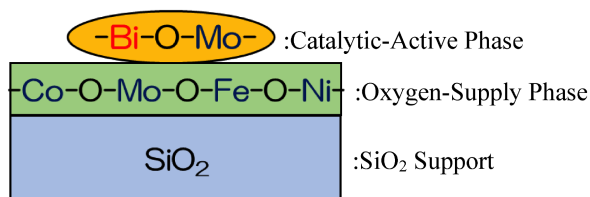
We previously showed that this catalytic process consists of two phases²¹⁾. The oxygen-supply phase for lattice oxygen involves Mo-oxide doping with transition metals such as Fe, Ni and Co supported on SiO₂. The catalytic-active phase for hydrogen abstraction from the reactant involves Bi–Mo oxide supported by the oxygen-supply phase, as shown in **Scheme 1**^{5),22)}. This concept is utilized in industrial catalysts.

We previously found that an insufficient supply of oxygen to the catalyst resulted in serious catalyst deactivation and inadequate activity²¹⁾. Therefore the present study tried to improve the redox property of the oxygen-supply phase *via* doping with cerium species. The redox property of the catalyst is improved by dop-

DOI: doi.org/10.1627/jpi.63.267

* To whom correspondence should be addressed.

* E-mail: sugiyama@tokushima-u.ac.jp



Scheme 1 Schematic Illustration of the Catalyst Concept Used in the Present Study

ing with various transition metals. The effect of adding cerium to the oxygen-supply phase was examined because of the remarkable redox and oxygen storage capacity (OSC) properties. The advantageous effect of cerium addition has been reported for Ag-Mo-PO catalysts in the reaction of propane to form acrolein²³, but not for bismuth molybdenum-based oxide catalysts for the conversion of propylene to acrolein.

2. Experimental

2.1. Catalyst Preparation

The preparation procedure followed that for silica-supported bismuth–molybdenum complex oxide catalyst^{16,17}. Cerium was doped first into the oxygen-supply phase supported on SiO₂, followed by the formation of a catalytic-active phase that consisted of the Bi-Mo-complex oxide in an oxygen-supply phase. Cerium was doped by replacing 0, 1, 3, 5, 10, 20 and 30 wt% of cobalt in the oxygen-supply phase. The catalytic-active phase was prepared under previously reported conditions that facilitated the formation of γ -Bi₂MoO₆. Among the various Bi-Mo composite oxides used for the partial oxidation of propylene to acrolein, α -Bi₂Mo₃O₁₂ is known to have a high level of activity for extracting the α -hydrogen of propylene, whereas γ -Bi₂MoO₆ can easily introduce gaseous oxygen into the catalyst⁷. The present study focused on the γ -type to improve the redox nature of the catalyst. The catalyst doped with 1 wt% Ce (hereafter, as referred to as 1 %-Ce catalyst) was prepared as follows. Iron(III) nitrate nanohydrate (0.931 g), cobalt(II) nitrate hexahydrate (2.849 g), nickel(II) nitrate hexahydrate (2.847 g), and cerium(III) nitrate hexahydrate (0.043 g) were dissolved in distilled water (7 mL) at 353 K. An aqueous solution consisting of hexaammonium heptamolybdate tetrahydrate (4.070 g) and distilled water (40 mL) was then added dropwise with stirring. These reagents were purchased from FUJIFILM Wako Pure Chemical Corp. and used as supplied. A silica-slurry (41.540 g; 20 wt% water dispersion) of hydrophilic fumed silica (8.308 g; AEROSIL® 50, Nippon Aerosil Co., Ltd.) was added into the resultant solution, followed by stirring at 338 K for 4 h. The final solution was dried at 373 K for 16 h under air-circulation. The resultant solid was finally calcined at 873 K for 2 h to

produce the 1 %-Ce oxygen-supply phase (1 %-Ce OSP). This 1 %-Ce OSP (3.034 g) and bismuth(III) oxide (1.534 g; FUJIFILM Wako Pure Chemical Corp.) were added to an aqueous solution of distilled water (3.6 mL), 28 % ammonia solution (0.5 mL), and hexaammonium heptamolybdate tetrahydrate (1.744 g), and was kneaded for 30 min. The resultant paste was dried at 403 K and calcined at 773 K for 6 h under air to obtain the 1 %-Ce catalyst.

2.2. Characterization of the Catalyst

The catalysts were analyzed using a SmartLab/R/INP/DX (Rigaku Corp.) and nitrogen adsorption-desorption measurement (BELSORPmax12, Microtac-BEL Corp.). The powder X-ray diffraction (XRD) patterns of the materials were obtained using monochromatized Cu K α -radiation (40 kV, 150 mA). Before the nitrogen adsorption-desorption measurement at 77 K, the catalysts were pretreated at 473 K for 5 h under vacuum. The BET surface area was calculated from the obtained isotherm. The surface properties of the materials were evaluated by X-ray photoelectron spectroscopy (XPS; PHI-5000VersaProbe II, ULVAC-PHI Inc.). The XPS spectra of the catalysts were obtained using Al K α -radiation and were calibrated based on a C 1s peak at 284.6 eV.

2.3. Evaluation of the Catalytic Performance

The catalytic activity tests were carried out in a fixed-bed continuous-flow reactor at atmospheric pressure²¹. Each catalyst (0.7 g) was pelletized and sieved to 0.85–1.70 mm, fixed with quartz wool, and pretreated with 25 mL/min of O₂ gas flow at 623 K for 1 h. After the pretreatment, catalytic activity tests were started at 623 K by passing 15 mL/min of a gas mixture of helium, propylene and oxygen through the reactor. Partial pressures were adjusted to $P(\text{C}_3\text{H}_6) = 10.1$ kPa, and $P(\text{O}_2) = 0, 15.5, \text{ or } 31.0$ kPa, and then diluted with He. Under these conditions, any homogeneous-gas phase reaction was negligible.

The reaction was monitored using a gas chromatograph (GC-8APT, Shimadzu Corp.) equipped with a thermal conductivity detector (TCD) and a capillary gas chromatograph (GC-2025 or GC2010, Shimadzu Corp.) equipped with a hydrogen-flame ionization detector (FID). The GC-8APT used a Molecular Sieve 5A (0.2 m \times ϕ 3 mm) column for O₂, CH₄, and CO and a Porapak Q (6.0 m \times ϕ 3 mm) column for CO₂ at 318 K. The GC-2025 used an Rt@-Alumina BOND/Na₂SO₄ capillary column (30 m \times ϕ 0.53 mm, Restek Corp.) for the C2 and C3 species at 403 K. The GC-2010 used a Stabilwax capillary column (30 m \times ϕ 0.25 mm, Restek Corp.) for the C3 species, acetaldehyde, propylene oxide, propionaldehyde, acetone, and acrolein at 313 K. The carbon balance between the reactant and the products was within ± 5 %. Product selectivity and propylene conversion were calculated on the C1 basis.

3. Results and Discussion

3.1. Characterization of Fresh Catalysts

The specific surface areas of the 0-, 1-, 3-, 5-, 10-, 20-, and 30 %-Ce catalysts were 21, 21, 22, 21, 18, 17, and 19 m²/g, respectively. The XRD patterns of fresh 0-, 10-, 20-, and 30 %-Ce catalysts are shown in Fig. 1.

The XRD patterns were essentially identical for all Ce-loading, and showed α -Bi₂Mo₃O₁₂ (PDF 01-078-2420), γ -Bi₂MoO₆ (PDF 01-077-1246), MoO₃ (PDF 01-074-7382), (Co_{0.7}Fe_{0.3})(MoO₄) (PDF 01-089-6590), and Bi₂O₃ (PDF 01-080-9185). As expected, γ -Bi₂MoO₆ was the main component. However, XRD patterns from Ce- and Ni-containing species were not detected, probably due to the low loadings. XRD signals due to CeO₂ (PDF 01-080-5549) were expected, but were overlapped by the corresponding signals due to (Co_{0.7}Fe_{0.3})(MoO₄).

3.2. Effects of Cerium Doping on Catalytic Activity

Figure 2 shows the catalytic performances for various Ce catalysts at $P(\text{O}_2) = 31.0$ kPa and 623 K. Clearly only the 0 %- and 10 %-Ce catalysts underwent catalytic deactivation. Furthermore, the selectivity and yield for acrolein at 6 h on-stream were enhanced from 28.9 % and 27.7 % on the 0 %-Ce catalyst to 71.2 % and 61.8 % on the 20 %-Ce catalyst. Additional enhancement of the activity was not detected with the 30 %-Ce catalyst. Such clear evident enhancement of catalytic activity was not detected at $P(\text{O}_2) = 15.5$ kPa, at which the values for selectivity and yield of acrolein at 69.7 % and 57.6 % on the 0 %-Ce catalyst at 6 h on-stream were slightly enhanced to 77.1 % and 65.3 % on the 20 %-Ce catalyst (Table 1). In addition to the values shown in Fig. 2 and Table 1, C₂H₄, C₃H₈, acetaldehyde and propionaldehyde were obtained with a selectivity of ca. 1 %. To investigate the effect of Ce

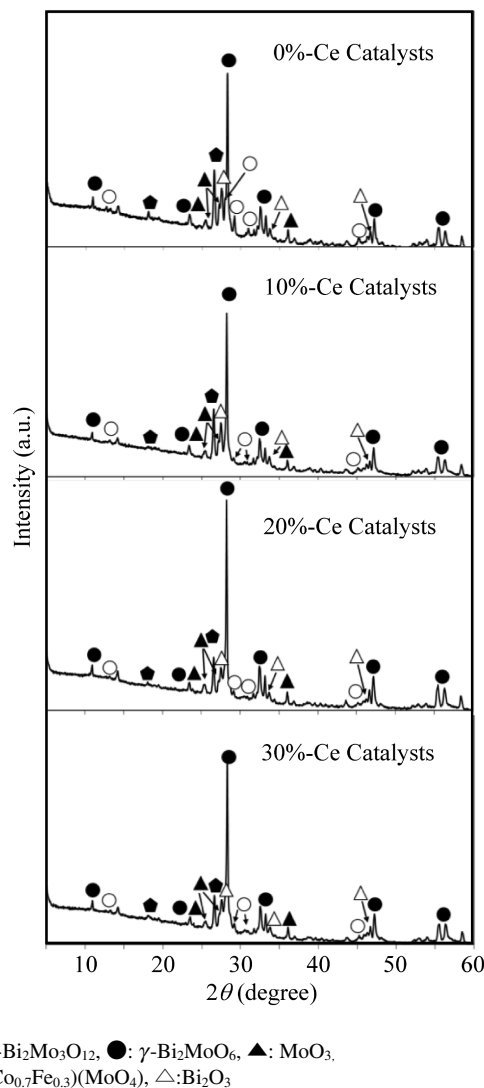


Fig. 1 XRD Patterns of Fresh 0 %, 10 %, 20 %, and 30 %-Ce Catalysts

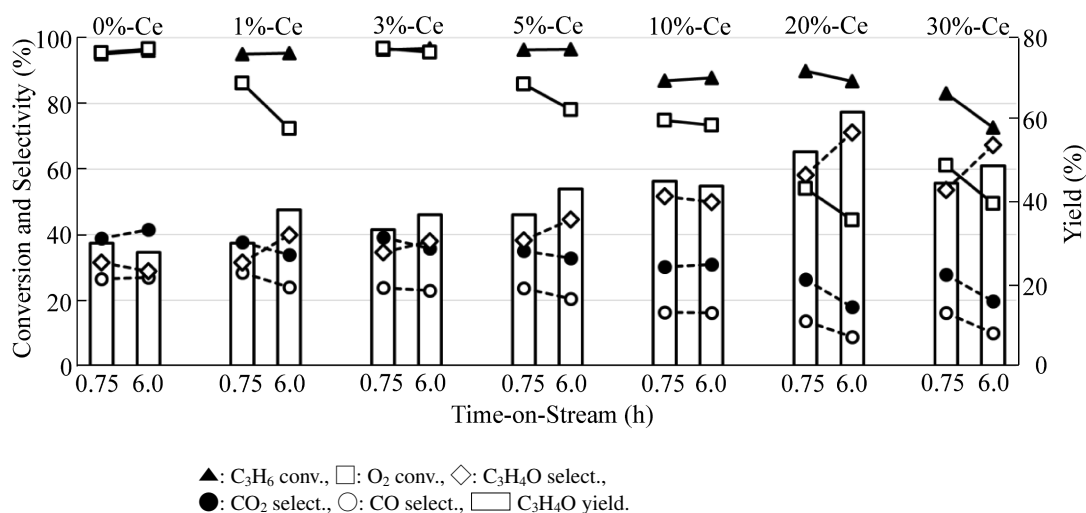


Fig. 2 Catalytic Activity on Various Ce Catalysts at $P(\text{O}_2) = 31.0$ kPa and 623 K

Table 1 Conversion, Selectivity, and Yield on Various Catalysts at $P(\text{O}_2) = 15.5$ kPa and 623 K

Catal.	Conv. [%]		Select. [%]			Yield [%]
	C_3H_6	O_2	$\text{C}_3\text{H}_4\text{O}$	CO_2	CO	$\text{C}_3\text{H}_4\text{O}$
0 %-Ce	81.6	89	70.7	19.2	6.8	57.7
	82.6	87	69.7	20.2	7.1	57.6
1 %-Ce	78.2	95	72.1	18.6	6.4	56.4
	77.8	86	68.5	21.3	7.6	53.3
3 %-Ce	78.6	86	73.8	17.3	6.5	58.0
	71.1	95	74.2	18.2	6.1	52.8
5 %-Ce	82.7	96	73.5	17.3	6.1	60.8
	83.3	97	73.0	17.3	6.5	60.8
10 %-Ce	86.0	88	75.7	15.2	5.4	65.1
	87.0	94	73.4	17.1	6.4	63.8
20 %-Ce	82.9	70	77.5	14.2	5.9	64.2
	84.6	86	77.1	14.9	5.5	65.3
30 %-Ce	67.2	85	74.6	17.2	5.6	50.1
	77.2	85	66.2	22.2	9.0	47.8

Upper and lower values for each catalyst show data at 0.75 h and 6.0 h on-stream, respectively.

Table 2 Catalytic Activities on 0 %-Ce and 10 %-Ce Catalysts in the Absence of Oxygen

Catal.	TOS ^{a)} [min]	Conv. [%] C_3H_6	Select. [%]		
			$\text{C}_3\text{H}_4\text{O}$	CO_x	C_3H_8
First experiment after pretreatment with O_2					
0 %-Ce	3	10.8	9.0	84.9	2.5
	35	0.5	5.3	44.5	22.0
10 %-Ce	3	8.4	13.5	81.8	0.0
	35	0.3	2.7	0.0	61.6
Second experiment after first re-oxidation with O_2					
0 %-Ce	3	8.2	14.4	76.5	2.6
	35	0.5	1.4	28.2	51.7
10 %-Ce	3	4.0	25.6	58.1	4.6
	35	0.5	2.0	30.1	35.4
Third experiment after second re-oxidation with O_2					
0 %-Ce	3	10.9	8.9	83.4	3.6
	35	2.2	0.0	49.3	33.1
10 %-Ce	3	5.5	20.0	68.8	2.9
	35	0.4	2.1	24.0	36.7

a) Time-on-stream.

doping on the present reaction, we focused on the unique reductive ability of Co and Ce oxides. Co_3O_4 is easily reduced to metallic Co with H_2 at around 623 K²⁴). However, CeO_2 is reduced gradually to Ce_2O_3 , but not metallic Ce, at wider temperature ranges between 573 K and 1123 K with H_2 . Therefore, doping with Ce reduces the ability for extraction of lattice oxygen from the catalyst, which is equivalent to the reductive ability of the catalyst.

Consequently, Ce-doping increases the catalytic activity under higher partial pressure of oxygen at 31.0 kPa. We suggest that conversion of acrolein to

CO_x is suppressed due to the decrease in the reductive ability of the catalyst *via* Ce-doping, which results in higher selectivity for acrolein at $P(\text{O}_2) = 31.0$ kPa on the 20 %-Ce catalyst. As expected, excess doping with 30 %-Ce resulted in a decreased catalytic activity.

3.3. Catalytic Activity in the Absence of Oxygen

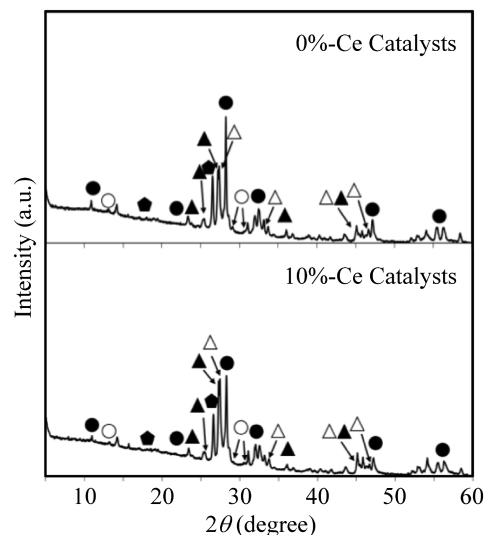
The catalytic activities of 0 %- and 10 %-Ce catalysts in the absence of oxygen in the feed stream at 623 K are described in **Table 2**. 30 %-Ce catalyst was excluded since the activity was rather low as shown in **Fig. 2** and **Table 1**. We decided to further examine the 10 %-Ce catalyst, since 20 %-Ce might resemble

30 %-Ce catalyst.

With the exception of the supply of O_2 in the feed stream, the activity test was performed using the usual experimental conditions such as $W = 0.7$ g, $T = 623$ K, $F = 15$ mL/min, $P(C_3H_6) = 10.1$ kPa, and $P(O_2) = 0$ kPa. Then used catalyst was re-oxidized using gaseous oxygen for 1 h at the specified reaction time, followed by a second activity test in the absence of O_2 , second re-oxidation, and a third activity test in the absence of O_2 . The reaction was monitored till 125 min on-stream, but **Table 2** shows the results at 3 min and 35 min on-stream, since the activity disappeared after shorter time-on-stream, regardless of doping with Ce. Production of propane became remarkable as the time-on-stream became longer in each case. The results of the reaction in the absence of oxygen in the feedstream are shown in **Table 2**. Therefore, if active oxygen is not abstracted from the catalyst, acrolein and CO_x cannot be produced. However, as is clear from **Table 2**, acrolein and CO_x were produced, indicating that the lattice oxygen of the catalyst was extracted to participate in the partial oxidation of propylene. Under these conditions, water is produced, and carbon deposition on the catalyst surface becomes remarkable. Hydrogen and CO_x are generated from the reaction between water and carbon deposition, both formed as above. As this hydrogen reacts with propylene, propane is generated. Longer time-on-stream results in more propane produced as shown in **Table 2**, as the above discussion suggests. After re-oxidation, catalytic activity on the 0 %-Ce catalyst was almost recovered, even in the third test. In contrast, catalytic activity of the 10 %-Ce catalyst only recovered to about half in the second and third tests. Although the activity was improved to some extent by re-oxidation, the catalyst structure was not expected to change significantly.

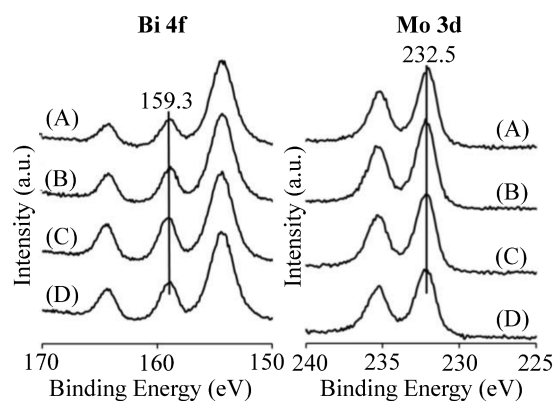
However, the structure of the catalyst obtained after the second re-oxidation, as shown in **Table 2**, was considerably collapsed compared with **Fig. 1**. α - $Bi_2Mo_3O_{12}$, γ - Bi_2MoO_6 , $(Co_{0.7}Fe_{0.3})(MoO_4)$, MoO_3 , and Bi_2O_3 , which also appear in **Fig. 1**, were detected from both catalysts after the second round of re-oxidation as shown in **Fig. 3**. The intensity due to the signals from γ - Bi_2MoO_6 , which was the main component in these fresh catalysts (**Fig. 1**), became smaller, whereas the intensity of the signals due to the decomposition species from γ - Bi_2MoO_6 , such as MoO_3 and Bi_2O_3 , became greater.

Two XPS peaks due to Mo $3d_{3/2}$ and $3d_{5/2}$ appeared between 225 eV and 240 eV, and two smaller peaks due to Bi $4f_{5/2}$ and $4f_{7/2}$ together with one greater peak due to Si 2s appeared between 150 eV and 170 eV as shown in **Fig. 4**²⁵. Clearly the state of Bi and Mo on the outermost surface region of the catalyst was maintained regardless of either the usage history or the loading of Ce. This result indicates that even if lattice oxygen is



○: α - $Bi_2Mo_3O_{12}$, ●: γ - Bi_2MoO_6 , ▲: MoO_3 ,
◆: $(Co_{0.7}Fe_{0.3})(MoO_4)$, △: Bi_2O_3 .

Fig. 3 XRD Patterns of 0 %- and 10 %-Ce Catalysts after a Second Re-oxidation



(A) Fresh 0 %-Ce catalyst, (B) 0 %-Ce catalyst after a second re-oxidation, (C) fresh 10 %-Ce catalyst, and (D) 10 %-Ce catalyst after a second re-oxidation.

Fig. 4 XPS Patterns due to Bi 4f and Mo 3d from Samples Used in the Results Shown in Figs. 1 and 3 for 0 %-Ce and 10 %-Ce Catalysts

extracted from the outermost surface of the catalyst, the formed vacancy can be supplemented using lattice oxygen from the oxygen-supply phase, and the state of the surface is maintained during the reaction. Therefore, no deficiency of lattice oxygen occurs on the outermost surface of the catalyst, which results in the maintenance of the high level of activity.

The catalyst structure was extensively changed, but the deactivation behaviors were similar, regardless of the Ce-doping. Therefore, we expected the surface properties of the fresh catalysts to be retained following a second round of re-oxidation. To confirm this

expectation, the samples used in obtaining the results shown in **Figs. 1** and **3** for 0 %-Ce and 10 %-Ce catalysts were analyzed using XPS.

4. Conclusions

Introduction of cerium into the oxygen-supply phase of a Bi-Mo complex oxide catalyst supported on SiO₂ enhanced the selectivity and yield of acrolein and suppressed the catalytic activity for the partial oxidation of propylene to acrolein. These advantageous results were caused by the suppression of the reductive ability of the catalyst due to the introduction of cerium. In this study, the use of cerium with suitable redox properties effectively controlled oxygen abstraction in the oxygen-supply phase. Therefore, the concept of a catalyst preparation that focuses on the oxygen-supply phase and the catalytic-active phases is strongly supported.

Acknowledgment

This study was supported by the Research Clusters Program of Tokushima University (1702001), for which we are grateful.

References

- 1) Veatch, F., Callahan, J. L., Millberger, E. C., Forman, R. W., "2nd Actes Intern. Congr. Catalyse, Paris, 1960," Vol. II, 2647, Editions Technip., Paris (1961).
- 2) Voge, H. H., Adams, C. R., *Adv. Catal.*, **17**, 151 (1967).
- 3) Idol, J. D. Jr., U.S. Pat. 2904580 (1959), to Standard Oil (Ohio).
- 4) Grasselli, R. K., Burrington, J. D., *Adv. Catal.*, **30**, 133 (1981).
- 5) Moro-oka, Y., Ueda, W., *Adv. Catal.*, **40**, 233 (1994).
- 6) Keulks, G. W., Krenzke, D., Nothermann, T. M., *Adv. Catal.*, **27**, 183 (1978).
- 7) Le, M. T., Van Well, W. J. M., Stoltze, P., Van Driessche, I., Hoste, S., *Appl. Catal. A: Gen.*, **282**, 189 (2005).
- 8) Van Well, W. J. M., Le, M. T., Schiødt, N. C., Hoste, S., Stoltze, P., *J. Mol. Catal. A*, **256**, 1 (2006).
- 9) Schuh, K., Kleist, W., Høj, M., Trouillet, V., Beato, P., Jensen, A. D., Patzke, G. R., Grunwaldt, J., *Appl. Catal. A: Gen.*, **482**, 145 (2014).
- 10) Schuh, K., Kleist, W., Høj, M., Trouillet, V., Beato, P., Jensen, A. D., Grunwaldt, J., *Catalysts*, **5**, 1554 (2015).
- 11) Forzatti, P., Villa, P. L., Ferlazzo, N., Jones, D., *J. Catal.*, **76**, 188 (1982).
- 12) Ueda, W., Moro-oka, Y., Ikawa, T., *J. Catal.*, **70**, 409 (1981).
- 13) Zhai, Z., Getsoian, A. B., Bell, A. T., *J. Catal.*, **308**, 25 (2013).
- 14) Sprenger, P., Sheppard, T. L., Suuronen, J., Gaur, A., Benzi, F., Grunwaldt, J., *Catalysts*, **8**, 356 (2018).
- 15) Bui, L., Bhan, A., *Appl. Catal. A: Gen.*, **546**, 87 (2017).
- 16) Teshigawara, T., Kanuma, N., Iwakura, T., Jpn. Pat. 4280797 (2009).
- 17) Kameo, H., Kajitani, H., Iwakai, K., Takeo, H., Orita, S., Takeuchi, T., PCT International Publication No. WO/2012/121300 (2012).
- 18) Inaba, Y., Onuki, S., Naito, K., Yoshida, J., Yamaguchi, T., Izumiyama, K., Jpn. Pat. 5982214 (2016).
- 19) Kurakami, T., Matsumoto, S., Sudo, A., Shiraishi, K., Hashiba, T., Jpn. Kokai Tokkyo Koho, P2018-140993A (2018).
- 20) Ito, M., Ito, H., Jpn. Kokai Tokkyo Koho, P2019-166521A (2019).
- 21) Sugiyama, S., Nagai, K., Nakao, Y., Baba, Y., Katoh, M., *J. Chem. Eng. Jpn.*, **50**, 641 (2017).
- 22) Grasselli, R. K., *Top. Catal.*, **21**, 79 (2002).
- 23) Zhang, X., Wan, H., Weng, W., Yi, X., *Catal. Lett.*, **87**, 229 (2003).
- 24) Liotta, L. F., Di Carlo, G., Pantaleo, G., Venezia, A. M., Deganello, G., *Appl. Catal. B: Environ.*, **66**, 217 (2006).
- 25) Briggs, D., Seah, M. P., "Practical Surface Analysis," 2nd Ed., Vol. 1, John Wiley & Sons, (1990).

.....

要 旨

プロピレンからアクロレインへの部分酸化触媒であるシリカ担持ビスマス-モリブデン複合酸化物へのセリウムの添加効果

杉山 茂^{†1)}, 三宅 未珂^{†2)}, 吉田 瑞穂^{†3)}, 中尾 友紀^{†2)}, 霜田 直宏^{†1)}, 加藤 雅裕^{†1)}

^{†1)} 徳島大学大学院社会産業理工学研究部応用化学系, 770-8506 徳島市南常三島町2-1

^{†2)} 徳島大学大学院先端科学技術教育部化学機能創生コース, 770-8506 徳島市南常三島町2-1

^{†3)} 徳島大学理工学部応用化学システムコース, 770-8506 徳島市南常三島町2-1

SiO₂に担持されたBi-Mo複合酸化物触媒へのCe添加の効果を、プロピレンのアクロレインへの部分酸化について検討した。本研究で検討した触媒は二つの相で構成されており、SiO₂に担持されたMo-酸化物にFe, Ni, Coを導入した格子酸素に対する酸素供給相、およびその周りに担持した反応物からの水素引き抜きを行うBiサイトを持つBi-Mo酸化物の触媒活性相の2相である。本研究では、酸素供給相の酸化還元性を高めるために、酸素供給相にCeを添加した。Ce添加による良好な結果は、酸素リッチの原料ガスを用いた際に観測された。たとえば、 $P(\text{C}_3\text{H}_8)=10.1\text{ kPa}$, $P(\text{O}_2)=15.5\text{ kPa}$, $T=623\text{ K}$, 通塔時間6時間において、Ceの添加率を0%から20%に増加させても、アクロレインの収率は57.6%から65.3%へわずかに増加した

だけであった。一方、同条件で、 $P(\text{O}_2)=31.0\text{ kPa}$ とした酸素リッチの条件では、Ceの添加率を0%から20%に増加させると、アクロレインの収率は27.7%から61.8%へと約2倍増加した。原料ガス中に酸素を加えずに反応を繰り返した後の触媒のXPS分析により、触媒活性相と酸素供給相の間のユニークな酸化還元挙動が確認され、触媒活性相の格子酸素は酸素供給相から補充されて、触媒活性相表面の状態が維持されることが明らかになった。これらのXPSによる結果と、酸素リッチ状態での酸素供給相へのCe添加の触媒活性への顕著な効果に基づいて、酸素供給相と触媒活性相からなる触媒調製方法の概念が正しいことを明らかにした。

.....